ARTICLE

OBC
www.rsc.org/obc

Calix[4]azacrown and 4-aminophthalimide-appended calix[4]azacrown: synthesis, structure, complexation and fluorescence signaling behaviour†

Sandip Banthia and Anunay Samanta*
School of Chemistry, University of Hyderabad, Hyderabad, 500 046, India.
E-mail: assc@uohyd.ernet.in; Fax: +91 40 2301 2460

Received 20th January 2005, Accepted 9th March 2005
First published as an Advance Article on the web 22nd March 2005

The synthesis and single crystal structure of 25,27-(diamidomonoazacrown-5)-calix[4]arene (**L**), calix[4]arene capped by a diamide bridge in the 1,3-position on the lower rim, which forms a supramolecular dimer in the solid state *via* intermolecular hydrogen bonding, are described. A 4-aminophthalimide (**AP**) fluorophore has been regioselectively linked to the secondary amino function of the azacrown unit with a dimethylene spacer to construct *N*-(4-aminophthalimidoethyl)calix[4]azacrown (**APL**), a fluorescent sensor, *via* a fluorophore–spacer–receptor architecture. Fluorescence quantum yield and lifetime of **APL** have been measured to be lower than those of the bare fluorophore (**AP**) due to the photoinduced intramolecular electron transfer (PIET) between the fluorophore and the receptor moieties of the molecule. In the presence of transition metal ions, fluorescence enhancement of **APL** is observed suggesting the binding of the metal ion to the sensor. Complexation properties of **APL** with transition metal ions are investigated using UV-vis spectroscopy. A 1 : 1 stoichiometry of the complex is determined from a Job plot and the corresponding association constants for the various metal ions are evaluated. Fe^{3+} and Cu^{2+} ions have the largest association constants ($K = 2.3 \times 10^5$ M^{-1} and 1.6×10^5 M^{-1} respectively) compared to other metal ions indicating that they form complexes selectively with **APL**.

Introduction

Calix[4]arenes[1] are highly specific ligands[2–4] and their potential applications as hosts and sensing agents for various analytes have received increasing interest.[5] With appropriate appended groups, azacrowns combining calix[4]arene framework are good candidates as probe molecules for various species as they selectively entrap specific metal cations not only through an electrostatic interaction between the hetero atoms of the azacrown loop and the target metal ions but also through the three-dimensional encapsulating assistance of the appended side arm on the nitrogen atom.[6] Although several calixarene based fluorescent sensors have already been designed,[7–10] not much attention has been given towards the development of fluorescent sensors for transition and heavy metal ions. Noteworthy is a paper by Kim *et al.* in which pyrene is attached to the calix[4]azacrown ether with a methylene spacer to prepare a calix[4]azacrown based fluoroionophore.[11] In the presence of metal ions, photoinduced intramolecular electron transfer (PIET) between the nitrogen atom of the azacrown moiety and the pyrene fluorophore was blocked and chelation enhanced fluorescence (CHEF) was observed. However, since the azacrown loop in this compound comprised ether units, it showed CHEF even in the presence of alkali and alkaline earth metal cations making the system non-selective.[11]

Many effective fluorescent sensors have been successfully developed for alkali, alkaline earth metal cations as well as for the d^{10} metal ion such as Zn^{2+}.[12–15] However, a great deal of effort is still invested in the construction of devices that are able to signal the presence of heavy and transition metal ions.[16,17] Considering the growing interest in molecules capable of performing logic operations,[18] special attention has to be focused on the importance of heavy and transition metal ions in such devices serving as molecular switches.[19–21] As transition metals and many heavy metals are known as fluorescence quenchers *via* enhanced spin–orbital coupling,[22] energy or electron transfer,[23] development of selective as well as sensitive fluorescent sensors for these metal cations presents a challenge.

We have chosen calix[4]azacrowns of a type in which the calix[4]arene is capped by a diamide bridge at the 1,3-position on the lower rim. ^{1}H NMR studies have previously indicated that macrocycles of this type show interesting binding properties.[24–26] While *p-tert*-butylcalix[4]azacrown does not extract transition metal ions, the corresponding 1,3-dimethoxy-*p-tert*-butylcalix[4]azacrown extracts Cu^{2+} ions selectively with respect to Co^{2+} and Ni^{2+} ions.[24,25] *N*-Methyl-1,3-dimethoxy-*p-tert*-butylcalix[4]azacrown, however, showed changes in its NMR spectrum in the presence of all three metal ions. Thus, a simple substitution by methyl groups leads to dramatic changes in the complexing properties of these systems. However, the measure of binding has not been studied in detail.[24,25] Complexation behaviour of related systems towards alkaline earth and transition metal ions and a crystal structure of the 1 : 1 complex with Mg^{2+} in which the metal is out of the crown loop were described recently.[26] In this report, we present the improved synthesis and the single crystal structure of calix[4]azacrown, **L**. A 4-aminophthalimide fluorophore has been regioselectively linked to the secondary amino nitrogen atom of compound **L** with a dimethylene spacer to obtain a fluorescent sensor, *N*-(4-aminophthalimidoethyl)calix[4]azacrown (**APL**). The photophysical, transition metal ion binding and the fluorescence signaling properties of **APL** have been described. Among the metal ions studied, this system is found to be selective for Fe^{3+} and Cu^{2+} metal ions.

Results and discussion

Compound **L** was synthesized by carrying out a condensation reaction of 1,3-*O*-dimethyl ester calix[4]arene (**1**)[27] and diethylenetriamine in a 1 : 1 mixture of toluene and methanol under reflux for 24 hours (Scheme 1). A general synthetic procedure, for calix[4]arenes capped by diamide bridges in the 1,3-position, employing 1,3-*O*-diethyl ester calix[4]arene

† Electronic supplementary information (ESI) available: tables of crystallographic information; thermal ellipsoid plots; NMR spectra; details of procedure for the estimation of the binding constant. See http://www.rsc.org/suppdata/ob/b5/b500912j/

DOI: 10.1039/b500912j

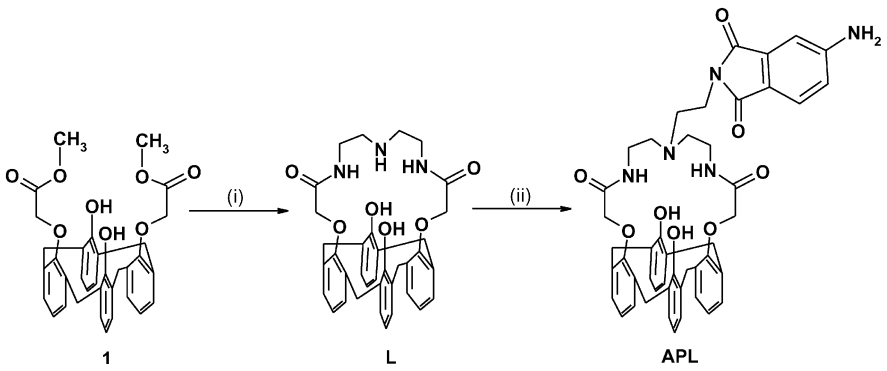

Scheme 1 Synthetic routes for the calix[4]azacrown **L** and the corresponding 4-aminophthalimide appended fluorescent sensor **APL**. Conditions: (i) diethylenetriamine, methanol–toluene, reflux, 24 h; (ii) *N*-bromoethyl-4-aminophthalimide, K_2CO_3, acetonitrile, reflux, 36 h.

have been described.[28] However, a minor modification of this procedure (see Experimental section for details) resulted in the reaction proceeding faster and with improved yield. The purified product, obtained as a white solid in 80% yield, adopts a cone conformation,[29] which is evident from the presence of an AB system at 3.46 ppm and 4.21 ppm (J = 13.5 Hz) characteristic of methylene bridges (ArCH_2Ar) and the position of the carbon atoms of the methylene bridges in the ^{13}C NMR at 31.14 ppm.[30]

A crystal structure analysis was used to probe the solid-state conformation. A single crystal of compound **L** obtained by slow evaporation of the methanol–chloroform solution crystallizes in the monoclinic space group $P2_1/n$. The asymmetric unit is composed of one calix[4]azacrown molecule in a cone conformation and a methanol molecule.[31] This combination gives strong hydrogen-bond donors and acceptors, which is reflected in the hydrogen-bonding network consisting of both intra- and intermolecular hydrogen bonds (Table 1). A polymorph of **L** was reported recently which crystallizes in a triclinic space group $P\bar{1}$.[32] Polymorphism of calixarene derivatives is emerging as a new area and will have implications in the field of calixarene chemistry.

The dihedral angles between the aromatic rings of the calixarene and the mean plane defined by the four methylene bridges are 35.18(17), 73.86(12), 40.21(14) and 75.95(12)°. The aromatic rings are tilted away from the calixarene cavity, the inter-planar angle between the two opposite rings are 75.39(17) and 30.20(18)°. This conformation leads to O···O separations of 4.654(4) Å between O(1) and O(3) and 3.202(5) Å between O(2) and O(4). The average O···O distance between adjacent oxygen atoms is 2.85 Å. The strong hydrogen-bonding network is the main conformation-determining feature of this molecule. While one phenolic proton is bound to an ether oxygen atom, the second one shows a bifurcated intramolecular hydrogen bond with a neighboring ether oxygen atom of the calixarene and an intermolecular hydrogen bond with the oxygen atom of a methanol molecule. Two intramolecular hydrogen bonds due to the amide protons are also bifurcated between the amide protons and the oxygen atoms bound to the calixarene. The proton of the amine function is bound to the amide oxygen atom of a neighbouring molecule leading to a supramolecular cyclic dimer in the solid state that is 'capped' at both ends by an association to the methanol molecule (Fig. 1).

Table 1 Hydrogen-bonding geometry (Å, °) in the crystal structure of **L**·CH_3OH

D–H···A	D–H	H···A	D···A	<D–H···A
O4–H4···O3	0.82	2.07	2.846(5)	157.8
O2–H2···O1	0.82	2.12	2.878(5)	154.0
O2–H2···O7	0.82	2.42	2.891(6)	117.7
N3–H3···O4	0.86	2.25	3.100(5)	170.3
N3–H3···O1	0.86	2.18	2.578(5)	108.1
N1–H1···O2	0.86	2.34	3.200(5)	174.1
N1–H1···O3	0.86	2.23	2.638(5)	108.8
O7–H7···N2	0.82	2.02	2.823(7)	164.3
N2–H2A···O6[a]	0.92(4)	2.14(4)	2.909(6)	140(4)

[a] Symmetry code: $2-x, -y, -z$.

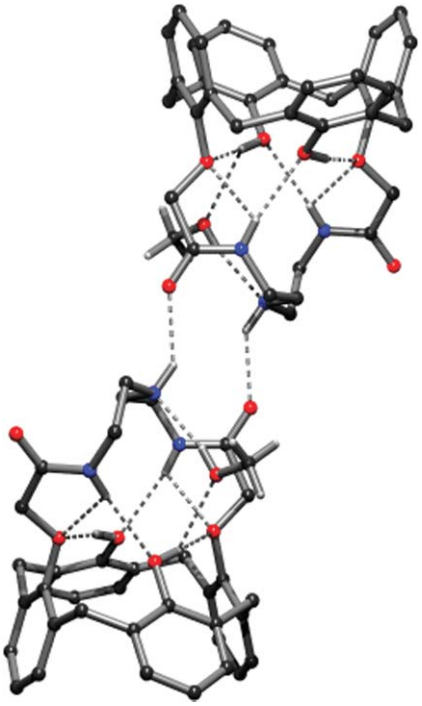

Fig. 1 View of the dimeric superstructure of **L** 'capped' with a methanol molecule illustrating the intra- and intermolecular hydrogen bonding, shown as dashed lines. Hydrogen atoms of **L** except those involved in H-bonding are omitted for clarity.

Since there exists considerable doubt about the metal extraction ability of a related *p-tert*-butylcalix[4]azacrown molecule,[24] we carried out the reaction between **L** and copper(II) perchlorate in methanol at room temperature (**CAUTION!** Care should be taken while treating organic compounds with metal perchlorates as potentially explosive mixtures may be formed). As expected, **L** did not form a complex with Cu^{2+} ions. Instead, it extracted the perchloric acid. Subsequent storage of the reaction mixture for slow evaporation yielded crystals, suitable for X-ray diffraction studies, of the calix[4]azacrown–perchloric acid complex (**L**·$HClO_4$). It crystallizes in the triclinic space group $P\bar{1}$. The asymmetric unit is composed of two independent calix[4]azacrown–perchloric acid and five disordered water molecules. The perchlorate motif is also highly disordered.[33] Thus, this proves that compound **L** exhibits poor complexation ability towards the transition metal ions. This

is in accord with observations for a corresponding *p-tert*-butylcalix[4]azacrown.[24] While compounds presenting labile-H protons were found to extract picric acid, *O*-methylated and *N*-methylated *p-tert*-butylcalix[4]azacrown were shown to complex transition metal ions as their picrates, suggesting that the complexing ability of calix[4]azacrowns is enhanced significantly upon substitution of the proton-ionizable atoms.[24,25] Taking this observation into consideration, an *N*-ethyl substituted 4-aminophthalimide fluorophore is substituted onto the amino functional group of the azacrown loop of **L** to obtain a fluorescent sensor, **APL**, with a fluorophore–spacer–receptor architecture (Scheme 1). The reaction between *N*-bromoethyl-4-aminophthalimide and **L** was carried out in acetonitrile in the presence of potassium carbonate at reflux for 36 h. The product was purified by column chromatography to obtain the pure compound, suitable for spectroscopic studies, in 25% yield and was characterized by CHN analysis, IR, ^{1}H and ^{13}C NMR and FAB mass spectrometry. The persistence of the cone conformation is confirmed by the presence of an AB system at 3.43 and 4.22 ppm (J = 13.5 Hz) for ArCH_2Ar protons and by the position of the carbon atoms of the methylene bridges in the ^{13}C NMR at 31.24 ppm. It is worth noting that the reaction afforded only the *N*-substituted product and the substitution on the phenolic OH could not be achieved even when a large excess of bromo compound was used. Thus, K_2CO_3 could be the base of choice for regioselective *N*-substitution of the secondary amine function in the bridging chain.

The absorption and fluorescence properties associated with the substituent (**AP**) moiety enable us to investigate the complexation properties in detail. The electronic absorption and fluorescence spectra of 4-aminophthalimide (**AP**) and **APL** in THF are shown in Fig. 2 and Fig. 3 respectively. Both systems exhibit broad intramolecular charge-transfer absorption and fluorescence bands. The fluorescence quantum yield of **APL** is measured to be 0.05 in THF, which is almost 14 times lower than that of the parent fluorophore (ϕ_f (**AP**) = 0.7 in THF).[34] Moreover, although the fluorescence lifetime of **AP** is reported to be 12.4 ns in THF,[34] **APL** exhibits multi-exponential decay behaviour (Fig. 4), with an average lifetime of 4.36 ns in THF. The photophysical data are listed in Table 2. A lower fluorescence quantum yield and a shorter fluorescence lifetime of **APL** compared to the bare fluorophore (**AP**) are clear indicators of photoinduced intramolecular electron transfer between the fluorophore and the calix[4]azacrown moieties of the molecule.

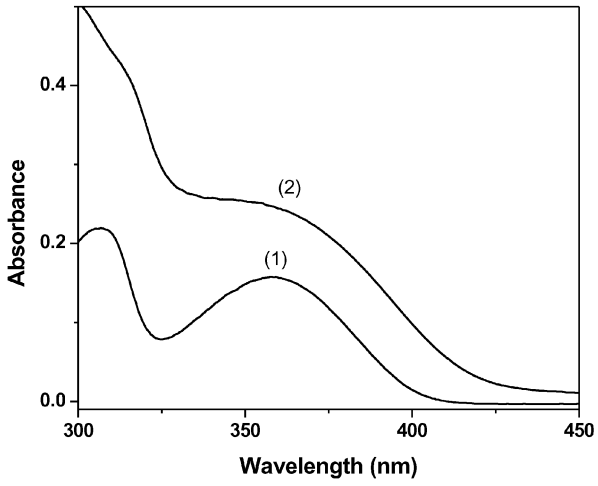

Fig. 2 Absorption spectra of (1) **AP** (4×10^{-5} M) and (2) **APL** (5.6×10^{-5} M) in THF.

Binding affinity of **APL** for transition metal ions in THF was investigated from the changes in the absorption spectrum of **APL** in the presence of these metal ions. The 4-aminophthalimide moiety in **APL** gives rise to a charge transfer transition in the UV-vis region due to the push–pull effect of the electron-donating amino and the electron-withdrawing carbonyl groups of the fluorophore. The changes in the absorption spectrum of **APL** in THF in the presence of the Cu^{2+} ions are shown in Fig. 5. As can be seen, addition of the metal salts leads to changes in the absorption spectrum. An isosbestic point over a certain concentration range can be observed. Among the metal ions studied, Mn^{2+} does not show any changes in the absorption spectrum of **APL**. In the presence of Ni^{2+} or Zn^{2+}, the absorption spectrum of **APL** is affected in a similar manner. However, the changes occurred at much higher concentration than those of Fe^{3+} and Cu^{2+}.

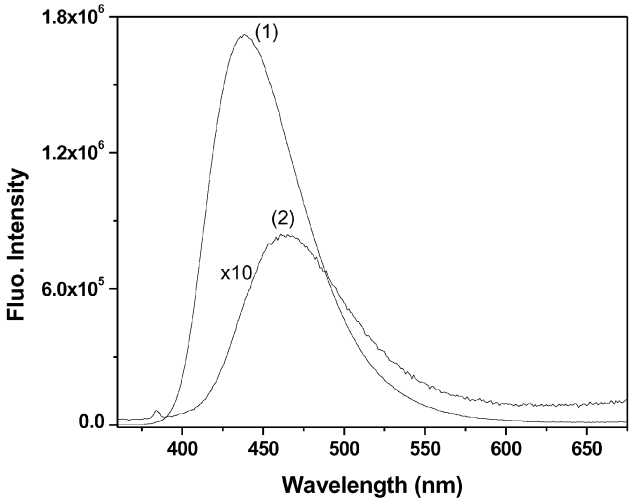

Fig. 3 Fluorescence spectra of (1) **AP** and (2) **APL** in THF. The solutions are optically matched at the excitation wavelength of 345 nm.

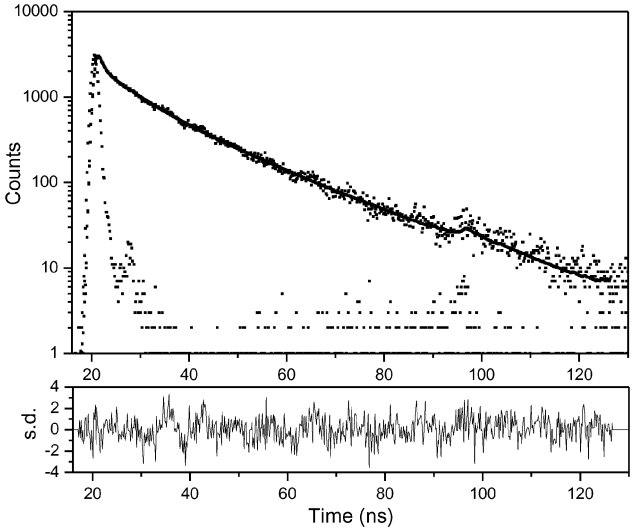

Fig. 4 Fluorescence decay behaviour of **APL** in acetonitrile. The solution was excited at 360 nm and the fluorescence was monitored at 470 nm. The data were fitted to a triexponential decay function with τ_1 = 0.58 ns (66%), τ_2 = 5.77 ns (17%), τ_3 = 17.32 ns (17%).

Table 2 Absorption and fluorescence[a] properties of 4-aminophthalimide (**AP**) and **APL** in THF

	λ_{max}/nm[b] (abs.)	λ_{max}/nm[b] (fluo.)	ϕ_f[c]	τ_f/ns[c]
AP[d]	357	445	0.70	12.40
APL	345	464	0.05	4.36[e]

[a] λ_{exc} = 345 nm. All fluorescence spectra were corrected for instrumental response. [b] ±2 nm. [c] ±10%. [d] These data were collected from ref. 34. [e] Average lifetime of the three components.

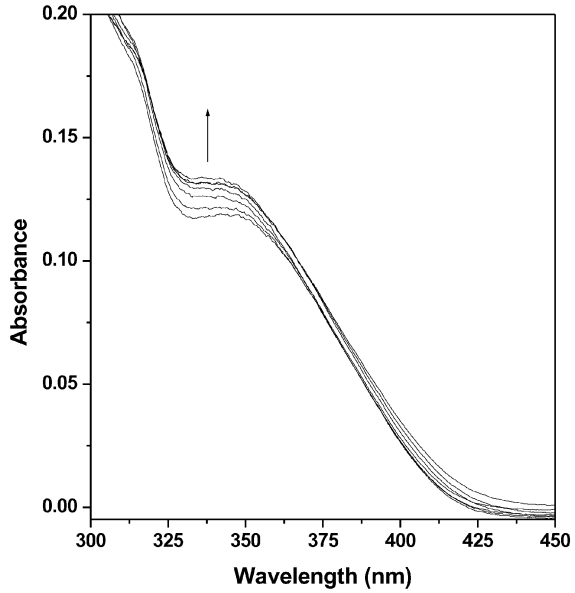

Fig. 5 Effect of Cu^{2+} ions on the absorption spectrum of **APL** (20 μM) in THF. The various concentrations of Cu^{2+} are 0, 3, 6, 9, 18, 27 and 39 μM.

In order to verify the 1 : 1 complexation, we used a Job plot experiment.[35] Fig. 6 illustrates that the **APL**–M^{n+} complex concentration approaches maximum when the molar fraction of $[M^{n+}]/([M^{n+}] + [\mathbf{APL}])$ is 0.5, suggesting that **APL** forms a 1 : 1 complex with these metal ions. Even though **APL** has multiple metal binding sites, it preferably forms the 1 : 1 complex presumably because the electrostatic repulsion between the two metal ions in the 1 : 2 complex is non-negligible.

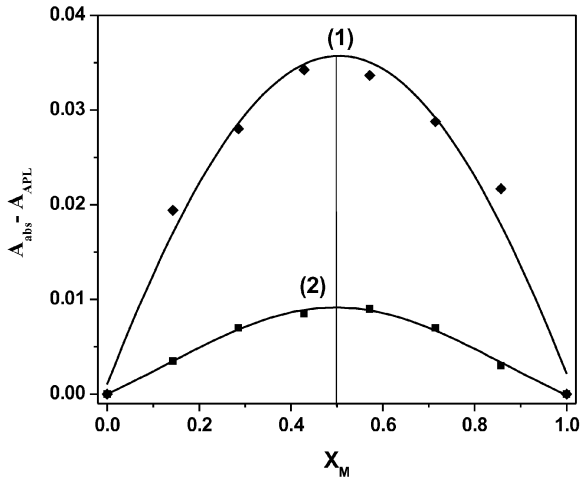

Fig. 6 Job plot of **APL** with (1) Cu^{2+} and (2) Ni^{2+} ions in THF. The variation of the absorption at 380 nm was measured as a function of the molar ratio $[M^{n+}]/([M^{n+}] + [\mathbf{APL}])$.

The association constant (K) of the complex is evaluated from the absorption data,[35] the details of the method are provided in the electronic supplementary information (ESI†). A typical plot from which the K value is evaluated is shown in Fig. 7. The linearity of the plot obtained further verifies the formation of the 1 : 1 complex and also suggests that the experimentally determined values of K are not uncertain. The K values (±10%), which were found to vary from 1.7×10^3 M^{-1} for Ni^{2+} to 2.3×10^5 M^{-1} for Fe^{3+} in THF, clearly indicate the selectivity of the present system towards binding with various transition metal ions (Table 3). Very high values of K for Fe^{3+} and Cu^{2+} compared to those for Ni^{2+} and Zn^{2+} ions make the present sensor system essentially sensitive and selective for Fe^{3+} and Cu^{2+} metal cations.

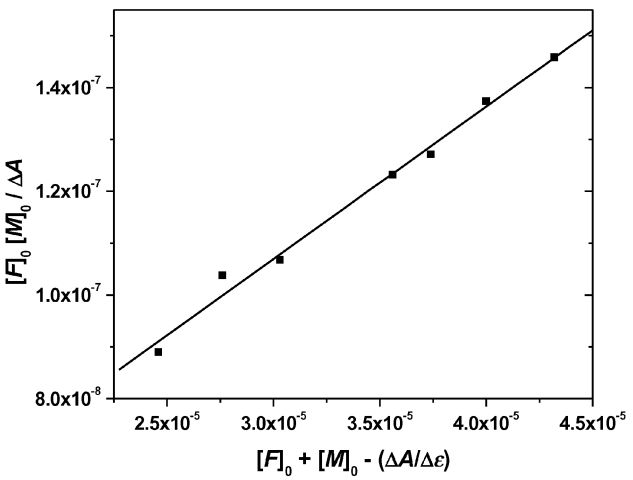

Fig. 7 A typical plot from which the association constant was estimated. The data shown in the plot are for Cu^{2+} in THF. The change in absorption is monitored at 380 nm. $[F]_0$ and $[M]_0$ are the initial concentration of **APL** and metal salt respectively. ΔA is the change in absorbance due to the addition of metal salts, and $\Delta\varepsilon$ is the difference between the molar extinction coefficient values of the complex and **APL**.

Table 3 Maximum fluorescence enhancement (FE) observed for **APL**[a] in the presence of different metal ions in THF

Metal ion[b]	$[M^{n+}]/10^{-5}$ M	K^c/M^{-1}	λ_{max}/nm	FE[d]
None	—	—	464	1
Fe^{3+}	2.0	2.3×10^5	482	2.5
Ni^{2+}	66	1.7×10^3	483	2.4
Cu^{2+}	3.9	1.6×10^5	487	2.8
Zn^{2+}	8.6	2.5×10^4	482	2.7

[a] Concentration $= 2 \times 10^{-5}$ M. [b] Hydrated perchlorate salts of the metals were used. [c] ±10%. [d] Samples were excited at the isosbestic point, ±10%.

Our attempts to determine the nature of the interaction between **APL** and the metal salt from NMR studies were not successful. With Fe^{3+} and Cu^{2+}, which form strong complexes, the NMR signals were too broad due to the paramagnetic nature of these ions. With diamagnetic Zn^{2+}, which does not form a strong complex, we could observe a shift of the NMR signals, particularly in the aromatic region. However, the spectra were too complex to interpret.

Addition of the metal salts leads to a Stokes shift of the fluorescence maximum and is associated with an enhancement of the fluorescence intensity of the system (Fig. 8). The fluorescence

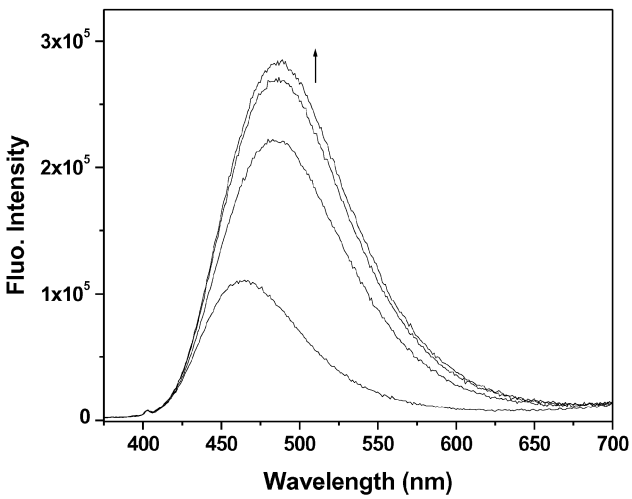

Fig. 8 Fluorescence spectra of **APL** (20 μM) in THF in the presence of Cu^{2+} ions. The concentrations of Cu^{2+} are 0, 18, 27 and 39 μM. Excitation was provided at 360 nm.

parameters of the system in the presence of the metal ions are collected in Table 3. Upon complexation, the communication between the receptor and the fluorophore moieties cuts "off" resulting into the inhibition of the PIET quenching pathway. The magnitude of the fluorescence enhancement (FE), which is a measure of the signaling efficiency of the present system, is found to vary between 2.4 and 2.8. Interestingly, FE in the presence of Fe^{3+}, a metal ion that has a d^5 electronic configuration and is known to be one of the most efficient fluorescence quenchers among the transition metal ions, is also observed. However, no enhancement of fluorescence was observed in the presence of Mn^{2+} ions indicating their inability to form a complex with the present system. Even though the magnitudes of FE observed in the presence of Ni^{2+} and Zn^{2+} ions are almost similar to those observed for Cu^{2+} and Fe^{3+} ions, the sensitivity and selectivity in the ion recognition by **APL** can be determined by observing the changes in the emission intensity as a function of the metal ion concentration. Both Ni^{2+} and Zn^{2+} modulate the fluorescence spectra in a similar fashion. However, the desired changes occur at a much higher concentration than those of Cu^{2+} and Fe^{3+} (Table 3). Thus, the modulation of the fluorescence spectra of **APL** in the presence of transition metal ions is in correlation with the selectivity trend observed from the UV-vis study.

In this context, it is important to take note of the fact that the metal salts used in this study are in their hydrated form and, hence, are acidic in nature. One can then argue that the fluorescence response of the sensor system in the presence of the metal salts is simply a reflection of the protonation of the amine nitrogen atom next to the fluorophore.[36] However, the very fact that no change of the fluorescence response of the system was observed in the presence of hydrated perchlorate salts of sodium and hydrated transition metal salts such as Mn^{2+} salts having a similar acidity strength[37] ensures that the proton is not the culprit and that **APL** has the ability to selectively coordinate Fe^{3+} or Cu^{2+} ions. Moreover, the high binding constant values ($\sim 10^5$ M^{-1}) for Fe^{3+} or Cu^{2+} ions compared to the other metal ions also rules out this possibility. Complexation and fluorescence signaling studies are also carried out in acetonitrile and water to investigate the effect of solvent. The results obtained in acetonitrile are similar to those observed in THF. In water, the "off–on" fluorescence signaling due to the metal ions or protons could not be observed because the PIET in **APL** is not efficient (evident from the similar values of fluorescence quantum yield of **AP** and **APL** in water).

We also examined the effect of the transition metal salts on the fluorescence decay behaviour of **APL**. The amplitude associated with the sub-nanosecond component of the fluorescence decay decreases significantly and a significant increase in the amplitude of the long component is observed on progressive addition of the metal salts. The amount of metal ion required to effect the above change depends on the association constants of various complexes. The greater the association constant, the smaller the amount of metal ion required. Thus, the selectivity among the metal ions is also observed by the change in the fluorescence lifetime values in the presence of metal ions. An increase in the lifetime of the system in the presence of the metal ions is in accordance with the metal ion-induced suppression of PIET in **APL**.

The present investigation indicates that while calix[4]-azacrown (**L**) does not extract transition metal ions, *N*-(4-aminophthalimidoethyl)calix[4]azacrown (**APL**) has the ability to bind with transition metal ions with certain amount of selectivity. Studies on the corresponding *p-tert*-butylcalix[4]azacrown revealed that metal complexing property of this type of calix[4]azacrown can be varied upon substitution on phenolic OH or both phenolic OH and amine NH.[24] Here, we find that substitution on only one amine NH can also make the system capable of binding with transition metal ions. The possible explanation for this observation can be rationalized on the basis of the hydrogen-bonding pattern found in this system. These systems, possessing donor and acceptor sites for hydrogen bonding, can behave as polydentate ligands capable of complexing neutral molecules containing OH or NH groups. As can be seen from the structure of **L**, a methanol molecule is encapsulated upon hydrogen bonding with the phenolic proton and amine nitrogen, which in turn is hydrogen-bonded to the neighbouring molecule to give a supramolecular dimeric structure (Fig. 1). As most of the metal salts are hydrated, it is highly possible that formation of a hydrogen-bonded complex with the neutral molecules such as water is favoured more than the metal ion complexation. However, upon substitution on phenolic OH and amine NH, complexation with the metal ions predominates due to the decrease in the number of donor sites for hydrogen bonding thereby making the azacrown loop more flexible and available for the metal cations.

In conclusion, we have synthesized a designer ligand calix[4]azacrown (**L**) and determined its solid state structure. The poor complexation properties of this type of calix[4]azacrowns are attributed to the highly ordered hydrogen-bonding pattern leading to a supramolecular dimeric structure. **L** has been appended to a 4-aminophthalimide fluorophore to develop a fluorescent sensor (**APL**) for transition metal ions based on a PIET mechanism. The complexation and signaling behaviour of **APL** towards transition metal ions are investigated in detail. The selectivity observed for Fe^{3+} and Cu^{2+} suggests that macrocycles based on a calixarene platform may act as versatile ligands for the selective recognition of metal cations. The results presented by us along with the observations of others[24,25] indicate that slight modification of this type of calix[4]azacrown framework may result into potential hosts for the selective recognition of transition metal ions.

Experimental

Synthesis

Reagent grade reactants and solvents were obtained from commercial suppliers and used as received. Starting materials **1** and *N*-bromoethyl-4-aminophthalimide were prepared as described in the literature.[27,38]

25,27-(Diamidomonoazacrown-5)-calix[4]arene (L). A solution of 25,27-di(phenoxy-acetic acid methyl ester)calix[4]arene (**1**) (0.233 g; 0.41 mmol) and diethylenetriamine (0.0824 g; 0.8 mmol) in 1 : 1 methanol–toluene (20 ml) were refluxed for 24 hours. After removal of the solvents, the crude mixture was precipitated with methanol to give the desired product **L** (80%) as a white solid. ν_{max}(KBr pellet)/cm^{-1} 3381 (OH), 1670 (C=O); δ_H (400 MHz, $CDCl_3$) 2.98 (4 H, t), 3.46 (4 H, d), 3.55 (4 H, t), 4.21 (4 H, d), 4.52 (4 H, s), 6.73–6.84 (8 H, m), 7.15 (4 H, d), 8.30 (2 H, t); δ_C (100 MHz, $CDCl_3$) 168.23, 152.42, 151.32, 132.15, 129.44, 129.03, 128.02, 126.09, 120.29, 74.91, 49.02, 40.22, 31.14.

***N*-(4-Aminophthalimidoethyl)-25,27-(diamidomonoazacrown-5)-calix[4]arene (APL).** To a solution of calix[4]azacrown (**L**) (0.0607 g, 0.1 mmol) in dry acetonitrile (25 mL) were added *N*-bromoethyl-4-aminophthalimide (0.242 g, 0.9 mmol), potassium carbonate (0.124 g, 0.9 mmol), and a catalytic amount of KI. The mixture was allowed to reflux under a nitrogen atmosphere for 36 h with constant stirring. Subsequently, the solvent was evaporated, and the solid residue was purified by column chromatography on neutral alumina using ethyl acetate–hexane as eluent to give the desired product **APL** (25%) as a yellow solid (Found: C, 69.21; H, 5.59; N, 8.98. Calc. for $C_{46}H_{45}N_5O_8$: C, 69.43; H, 5.66; N, 8.81%); ν_{max}(KBr pellet)/cm^{-1} 3362 (OH), 1703 (imide C=O), 1664 (amide C=O); δ_H (400 MHz, $CDCl_3$) 2.81 (2 H, t, NCH_2), 2.91 (4 H, t, NCH_2), 3.43 (4 H, d, ArCH_2Ar), 3.55 (4 H, t, NCH_2), 3.75 (2 H, t, NCH_2), 4.22 (4 H, d, ArCH_2Ar), 4.53 (4 H, s, OCH_2CO), 6.78–6.85 (9 H, m, ArH), 7.08–7.11 (5 H, m, ArH), 7.51 (1 H, d, ArH), 8.30 (2 H, t, CONH); δ_C (100 MHz, $CDCl_3$) 168.29,

167.99, 152.53, 151.31, 151.25, 146.26, 132.31, 129.45, 128.90, 128.09, 126.62, 124.85, 120.47, 117.68, 110.50, 74.81, 55.60, 55.20, 39.22, 38.92, 31.24; *m/z* (FAB-MS) 797 $(M + 2H)^+$.

Instrumentation and methods

The absorption and fluorescence spectra were recorded on a Shimadzu spectrophotometer (UV-3101PC) and a Spex spectrofluorimeter (Fluoromax-3), respectively. All fluorescence spectra were corrected for instrumental response. The fluorescence decay profiles were recorded on a single photon-counting spectrofluorimeter (IBH, model 5000). The instrument was operated with a thyratron-gated flash lamp filled with hydrogen at a pressure of 0.5 atm. The lamp was operated at a frequency of 40 kHz, and the pulse width of the lamp under operating conditions was ~1.2 ns. The lifetimes were estimated from the measured fluorescence decay curves and the lamp profile using a nonlinear least squares iterative fitting procedure.[39] The details concerning the instrument can be found elsewhere.[40] The goodness of the fit was evaluated from the χ^2 values and the plot of the residuals. IR spectra were recorded on a Jasco FT-IR/5300 spectrometer as KBr pellets. NMR spectra were recorded on a Bruker AVANCE 400 MHz spectrometer at ambient temperature and were referenced to the internal ^1H and ^{13}C solvent peaks. Fast atom bombardment (FAB) mass spectrometry was performed at Central Drug Research Institute (CDRI) with the use of *m*-nitrobenzyl alcohol as the matrix. The quantum yield of the sample was measured relative to that of 4-aminophthalimide ($\phi_f = 0.7$ in tetrahydrofuran).[34] The solvents used in this study were rigorously purified following standard procedures.[41]

Collection and reduction of X-ray data‡

Calix[4]azacrown ($L{\cdot}CH_3OH$). Crystals were grown from methanol–chloroform solution. A tiny single crystal (dimension 0.48 × 0.40 × 0.32 mm) was mounted on the tip of a glass fiber and then mounted on the goniometer. The X-ray data were collected on an Enraf-Nonius Mach-3 four circle CAD-4 diffractometer employing graphite monochromatized Mo Kα radiation ($\lambda = 0.71073$ Å) by the ω-scan method. Unit cell parameters were determined by least squares fit of 25 reflections having θ values in the range 5.41–10.17°. Intensities of three check reflections were measured after every 1.5 h during the data collection to monitor the stability of the crystals. XCAD4 was employed for the data reduction.[42] The structure was solved by direct methods and refined by full matrix least-squares and difference Fourier techniques with the SHELXS-97 and SHELXL-97 programs respectively.[43] A multipurpose crystallographic tool, PLATON, was used for molecular graphics.[44] All non-hydrogen atoms were refined anisotropically. The H atom attached to the amine nitrogen atom was introduced as found on the Fourier difference maps and refined with restraint N–H = 0.87 Å and a displacement parameter equal to 1.5 times that of the parent atom. All other hydrogen atoms were introduced geometrically and refined using a riding model with a displacement parameter equal to 1.2 (amide NH, CH, CH_2) or 1.5 (OH, CH_3) times that of the parent atom. Relevant crystallographic information is summarized in Table S1, and the thermal ellipsoid plot is shown in Fig. S1 (ESI†).

Calix[4]azacrown–perchloric acid complex ($2L{\cdot}HClO_4{\cdot}5H_2O$). Single crystals were obtained from the slow evaporation of the reaction mixture. A tiny single crystal (dimension 0.29 × 0.12 × 0.04 mm) was mounted on the tip of a glass fiber and transferred to a Bruker CCD X-ray diffraction system with graphite-monochromatized Mo Kα radiation ($\lambda = 0.71073$ Å) controlled by a Pentium-based PC running the SMART software package.[45] Data were collected at room temperature and the raw data frames were integrated by the SAINTPLUS program package.[46] The structure was solved by direct methods and refined by full matrix least-squares and difference Fourier techniques with SHELXTL.[47] Empirical absorption corrections were applied with the SADABS program[48] and the space group was determined by examining systematic absences and confirmed by the successful solution and refinement of the structure. A multipurpose crystallographic tool, PLATON, was used for molecular graphics.[44] All non-hydrogen atoms were refined anisotropically. H atoms attached to amine nitrogen atoms and water molecules were introduced as found on the Fourier difference maps and refined with restraint N–H = 0.87 Å and O–H = 0.82 Å, respectively, with a displacement parameter equal to 1.5 times that of the parent atom. Oxygen atoms of three water molecules were left isolated as the hydrogen atoms located were highly disordered and could not be placed accurately. All other hydrogen atoms were introduced geometrically and refined using a riding model with a displacement parameter equal to 1.2 (amide NH, CH, CH_2) or 1.5 (OH, CH_3) times that of the parent atom. Relevant crystallographic information is summarized in Table S2, and the thermal ellipsoid plot is shown in Fig. S2 (ESI†).

‡ CCDC reference numbers 257059 and 257060. See http://www.rsc.org/suppdata/ob/b5/b500912j/ for crystallographic data in CIF or other electronic format.

Acknowledgements

This work is supported by the Council of Scientific and Industrial Research (CSIR), UPE Program of the University Grants Commission (UGC) and the Department of Science and Technology (DST), Government of India. SB thanks CSIR for the Fellowship. The structure determination was performed at the National Single Crystal Diffractometer Facility (funded by the DST), School of Chemistry, University of Hyderabad, India.

References

1 C. D. Gutsche, *Calixarenes*, Royal Society of Chemistry, Cambridge, 1989.
2 V. Bohmer, *Angew. Chem., Int. Ed. Engl.*, 1995, **34**, 713.
3 A. Ikeda and S. Shinkai, *Chem. Rev.*, 1997, **97**, 1713.
4 H. Halouani, I. Dumazet-Bonnamour, M. Perrin and R. Lamartine, *J. Org. Chem.*, 2004, **69**, 6521.
5 D. Diamond and M. A. McKervey, *Chem. Soc. Rev.*, 1996, **25**, 15.
6 J. S. Kim, O. J. Shon, J. W. Ko, M. H. Cho, I. Y. Yu and J. Vicens, *J. Org. Chem.*, 2000, **65**, 2386.
7 T. Jin, K. Ichikawa and T. Koyama, *J. Chem. Soc., Chem. Commun.*, 1992, 499.
8 I. Aoki, T. Sakaki and S. Shinkai, *J. Chem. Soc., Chem. Commun.*, 1992, 730.
9 H.-F. Ji, G. M. Brown and R. Dabestani, *Chem. Commun.*, 1999, 609.
10 H.-F. Ji, R. Dabestani, G. M. Brown and R. A. Sachleben, *Chem. Commun.*, 2000, 833.
11 J. S. Kim, O. J. Shon, J. A. Rim, S. K. Kim and J. Yoon, *J. Org. Chem.*, 2002, **67**, 2348.
12 J. P. Desvergne and A. W. Czarnik, *Chemosensors of Ion and Molecular Recognition*, Kluwer Academic Publishers, Dordrecht, 1997.
13 A. P. de Silva, D. B. Fox, A. J. M. Huxley and T. S. Moody, *Coord. Chem. Rev.*, 2000, **205**, 41.
14 B. Valeur and I. Leray, *Coord. Chem. Rev.*, 2000, **205**, 3.
15 S. C. Burdette, C. J. Frederickson, W. Bu and S. J. Lippard, *J. Am. Chem. Soc.*, 2003, **125**, 1778.
16 L. Prodi, F. Bolleta, M. Montalti and N. Zaccheroni, *Coord. Chem. Rev.*, 2000, **205**, 59.
17 K. Rurack, *Spectrochim. Acta Part A*, 2001, **57**, 2161.
18 A. P. de Silva, H. Q. N. Gunaratne and C. P. McCoy, *Nature*, 1993, **364**, 42.
19 P. D. Beer, P. A. Gale and G. Z. Cheng, *Coord. Chem. Rev.*, 1999, **185–186**, 3.
20 L. Fabbrizzi, M. Licchelli and P. Pallavinci, *Acc. Chem. Res.*, 1999, **32**, 846.
21 A. P. de Silva, I. M. Dixon, H. Q. N. Gunaratne, J. T. Gunnlaugsson, P. R. S. Maxwell and T. E. Rice, *J. Am. Chem. Soc.*, 1999, **121**, 1393.

22 D. S. McClure, *J. Chem. Phys.*, 1952, **20**, 682.
23 A. W. Varnes, R. B. Dodson and E. L. Wehry, *J. Am. Chem. Soc.*, 1972, **94**, 946.
24 I. Oueslati, R. Abidi, P. Thuery, M. Nierlich, Z. Asfari, J. Harrowfield and J. Vicens, *Tetrahedron Lett.*, 2000, **41**, 8263.
25 R. Abidi, I. Oueslati, H. Amri, P. Thuery, M. Nierlich, Z. Asfari and J. Vicens, *Tetrahedron. Lett.*, 2001, **42**, 1685.
26 I. Oueslati, R. Abidi, P. Thuery and J. Vicens, *J. Inclusion Phenom.*, 2003, **47**, 173.
27 F. Unob, Z. Asfari and J. Vicens, *Tetrahedron Lett.*, 1998, **39**, 2951.
28 I. Bitter, A. Grun, G. Toth, B. Balazs and L. Toke, *Tetrahedron*, 1997, **53**, 9799.
29 C. Jaime, J. de Mendoza, P. Prados, P. M. Nieto and C. Sanchez, *J. Org. Chem.*, 1991, **56**, 3372.
30 The NMR data are in agreement with the reported values, see ref. 32.
31 The ORTEP drawing and the crystal data are provided as electronic supplementary information (ESI†) in Fig. S1 and Table S1, respectively.
32 K. No, H. J. Lee, K. M. Park, S. S. Lee, K. H. Noh, S. K. Kim, J. Y. Lee and J. S. Kim, *J. Heterocycl. Chem.*, 2004, **41**, 211.
33 The ORTEP drawing and the crystal data are provided as electronic supplementary information (ESI†) in Fig. S2 and Table S2, respectively.
34 T. Soujanya, R. W. Fessenden and A. Samanta, *J. Phys. Chem.*, 1996, **100**, 3507.
35 K. A. Connors, *Binding Constants*, Wiley, Chichester, 1987.
36 J. F. Callan, A. P. de Silva, J. Ferguson, A. J. M. Huxley and A. M. O'Brien, *Tetrahedron*, 2004, **60**, 11125.
37 F. A. Cotton and G. Wilkinson, *Advanced Inorganic Chemistry*, Wiley Eastern Limited, Chichester, 1976.
38 S. Banthia and A. Samanta, *J. Phys. Chem. B*, 2002, **106**, 5572.
39 D. V. O'Connor and D. Phillips, *Time-Correlated Single Photon Counting*, Academic Press, London, 1984.
40 R. Karmakar and A. Samanta, *J. Am. Chem. Soc.*, 2001, **123**, 3809.
41 D. D. Perrin, W. L. F. Armarego, and D. R. Perrin, *Purification of Laboratory Chemicals*, Pergamon Press, Oxford, 1980.
42 K. Harms and S. Wocadlo, XCAD4, University of Marburg, Germany, 1995.
43 G. M. Sheldrick, SHELXS97 and SHELXL97, University of Gottingen, Germany, 1997.
44 A. L. Spek, PLATON, Utrecht University, Utrecht, The Netherlands, 1998.
45 SMART, 5.629 edn., Bruker AXS, Inc., Madison, WI, 2003.
46 SAINTPLUS, 6.45 edn., Bruker AXS, Inc., Madison, WI, 2003.
47 SHELXTL, 6.14 edn., Bruker AXS, Inc., Madison, WI, 2003.
48 SADABS, 2.10 edn., Bruker AXS, Inc., Madison, WI, 2003.